Motor Imagery Signal Classification: Insights from classical Time-Frequency Analysis of EEG Data

Erlend Withammer-Ekerhovd and Tore Gude

***Abstract*—This study presents an in-depth analysis of Motor Imagery (MI) signals using classical time-frequency analysis, with a focus on EEG data classification. Utilizing a dataset from the Institute of Neural Engineering, Graz University of Technology, comprising EEG data from 13 subjects, the research investigates two distinct classes of MI tasks. The primary objective is to explore the intricacies of MI signals, particularly in distinguishing between hand and feet movements. This is achieved through a comprehensive application of Multivariate Variational Mode Decomposition (MVMD) and Event-Related Desynchronization/Synchronization (ERDS) analysis. The study highlights significant subject-specific variability in EEG signals, emphasizing the challenges in classifying these signals. The findings reveal that lower frequency ranges in ERPs are critical for analyzing motor movements, yet exhibit considerable variability across subjects. The study sets a foundation for future research, particularly in addressing optimization of classification algorithms for MI signals.**

***Index Terms*—EEG, Motor Imagery, Signal Analysis, MVMD, ERDS, Spectrogram.**

The source code for the project is available at this GitHub repository.

I. Introduction

Motor Imagery (MI) can be defined as the mental rehearsal of an action without the actual movement being performed. The representation of the movement is rehearsed in the working memory and are being used in clinical settings, where patients have lost coordination and need to re-learn some movements to regain daily functionality [1]. MI has also been confirmed to have positive effects on training in other areas, such as education, medicine, music and sports [2]. The data set used for analysis in this report is an open access data set from Institute of Neural Engineering, Graz University of Technology. The data set consists of EEG data from 13 subjects and consists of two different classes of MI tasks, 5-second sustained movement of the right hand, class 1, and of the feet, class 2, as instructed by a cue. A single run consists of 20 trials. 100 trails were recorded from each person, 50 for each of the classes. The data set was originally recorded to train the machine learning technique Random Forest to classify the movements. This report addresses the use of classical time-frequency analysis to recover artifacts in a MI signal from this data set, that can be used to distinguish between hand and feet movement, which may later be extended for use in various machine learning techniques to perform the classification.

Classifying MI signals is a challenging task, as the signals often have a poor signal-to-noise ratio. The MI signals are also vulnerable to other muscular activity, such as eye blinks or bodily movements. With the emerging popularity of machine learning techniques, researchers have recently developed data-driven methods to classify MI signals, such as in [3]. Here, a Support-Vector Machine classifier were implemented to classify five classes of MI signals. The signals were pre-processed using a Filter Bank Common Spatio-Spectral Patterns technique.

Deep learning have also been researched as a method to classify MI signals. Convolutional Neural Networks have been the most widely used deep learning technique found in articles during the period 2017-2021. Different time-frequency techniques have been used to prepossess the EEG signals to be able to train the networks efficiently [4].

II. Methodology

A. Time-locked vs Phase-locked

To fully understand EEG analysis, it is important to understand the concepts of time- and phase-locking.

Time-locking is a crucial tool in understanding how brain activity changes with respect to an event, like a cue. This involves analyzing how the brain activity changes before, during and after the event occurs.

Phase is the concept of where in the cycle a wave is. It could be at the peak, at the trough, or somewhere in between. This is often visualized as a dot moving around a circle.

Phase-locking means that the phase of a particular frequency band is at the same point in the cycle at a specific time relative to an event. Crucially this time could change between events, however for a frequency band to be categorized as phase-locked the phases need to always align after a cue at some point in time.

These key differences lay the foundation for the differences between Event-Related Potential (ERP) and Event-Related Desynchronization (ERD)/Event-Related Synchronization (ERS) [5] [6].

B. Event Related Potential

For robust time-frequency analysis of the EEG signals, prepossessing of the data is necessary. The brain is constantly producing potentials and almost every sensory, mental or motion events may have the potential to cause transient response in the measured EEG signals if they are strong enough [7]. The potentials stemming from a given event, like a cue, are referred to as ERPs, and are time locked to the events [8]. The event in the data sets used are the cue indicating right hand or feet movement. However, EEG signals are often also contaminated by noise from many different sources, for example, facial muscular activity [9]. This makes it hard to distinguish the features of interest from noise in a single EEG event [10]. In

the data set used, some preprocessing of the data had already been done, such as notch filtering at 50 Hz removing noise from the electrical grid [11].

To improve the signal-to-noise ratio, different methods have been developed to help extract event-related brain response. ERP is obtained by averaging the EEG signals following repeated events given by the same cue. Epochs around the cue are created so that the moment of the cue are the same for each epoch before averaging the EEG signals. This is important so that the averaging of the EEG signals does not provide shifted results. In this signal averaging, the random noise in the EEG signal decreases while the ERP waveform increases, leading to extraction of the event-related activity. As the ERP is essentially an average, only the time- and phase-locked components remain after averaging for sufficiently large data sets. The resulting latency and amplitude of the signal are used to further analysis of the neural processing of the cue. [12].

In the data set used in this project, 100 trials per subject were recorded. For each trial, an epoch of one second before and after the 5-second-long cue were created and averaged due to their respective cue. This gave two resulting ERPs per channel, one belonging to the cue hand and one belonging to the cue feet. In total, for all the 15 channels, 30 ERPs were related to each of the 13 subjects.

When using averaging as a method to reduce the signal-to-noise ratio, one must also be aware that averaging over epochs and different trials leads to loss of information. Some features may be lost during averaging, and information about cross-trial variation of the event-related brain response signals are also lost in the process [13]. The ERP analysis in this project is done in Python using the MNE library.

C. Event-Related Desynchronization and Synchronization

ERD and ERS, combined ERDS, is an analysis tool used on time-locked EEG signals. While the ERP is both time- and phase-locked, ERDS are not phase-locked to an event and have different attributes and advantages for EEG analysis, like being highly frequency-band specific. ERD refers to a decrease in power in a specific frequency band following an event. This decrease is thought to reflect an increase in cortical activity in reference to the task. For MI this activity can be seen in the Motor Cortex. ERS on the other hand, refers to an increase in power, and a decrease in cortical activity like returning to a resting state [14]. The ERDS implementation is done in Python using the MNE and Seaborn libaries.

D. Multivariate Variational Mode Decomposition

Empirical Mode Decomposition (EMD) was presented by Huang et al. [15] and decomposes nonlinear and non-stationary data into a finite and often small number of Intrinsic Mode Functions (IMFs). Minima and maxima of the mother wave are recursively detected and interpolated to create upper and lower envelopes. The algorithm subtracts the mean of the upper and lower envelope recursively on the signal, which is then called the residual. This sifting process continues until the mean of the upper and lower envelope of the residual is 0 and the number of extrema of the residual are equal to the number of its zero-crossings ± 1. In this way, the EMD algorithm works as a way of recursively removing the highest frequencies of a signal. EMD is known to be sensitive to noise and sampling.

To improve the EMD algorithm to these sensitivities, Dragomiretskiy et al. [16] proposed an algorithm called Variational Mode Decomposition (VMD). VMD, as EMD, separates a signal into different modes. Each mode is narrowband. VMD tries to find the best set of modes, that are as smooth as possible, and are able to reproduce the original signal.

Multivariate Variational Mode Decomposition (MVMD) is an extension of the VMD algorithm to multichannel data [17]. As the data set have data recorded from 15 channels, MVMD is therefore chosen in this report to incorporate the multichannel information and provide a more comprehensive analysis of the data. MVMD decomposes a multichannel signal into the narrowband modes, that have a common frequency across all channels. Ideally, the obtained modes have minimum bandwidth, thus include few frequencies in each mode. MVMD is based upon that the signals that have common frequency components in all channels make up the multivariate modulated oscillations. The code for MVMD analysis is implemented in MATLAB utilizing the functions authored by [18].

E. Power Spectral Density and Spectrogram

Power Spectral Density (PSD) analysis is a method to analyze the distribution of power over frequencies for finite time series data [19]. The PSDs in this report are calculated in MATLAB using the function `pwelch`, which return the PSD using Welch's overlapped segment averaging estimator.

A spectrogram is a method that allow the representation of the frequencies component of a signal as they vary with time, thus being a time-frequency analysis tool [20]. The spectrograms in this report are calculated in MATLAB using Short-Time Fourier Transform (STFT).

F. Electrode Placement

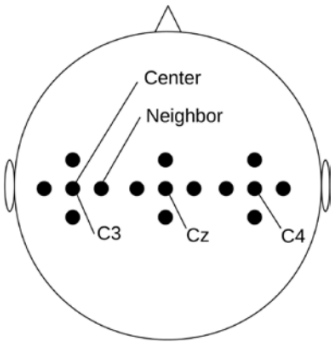

Fig. 1. Electrode placement on the scalp during recording of the data set.

The electrode placement follows Figure 1. With the numbering going from 1 to 15, from left to right, from front to back. This means channels 1, 2, and 3 are the front most channels, while 13, 14 and 15 are the back most channels. Channel 5 is C3, channel 8 is Cz and channel 11 is C4 [11].

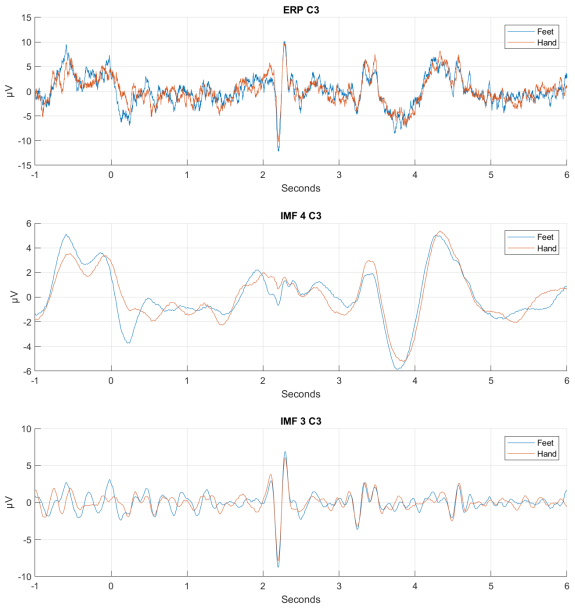

Fig. 2. MVMD result from the ERP for both hand and feet cues of C3. Only the two last IMFs are shown together with the ERP, with IMF 4 being the final IMF.

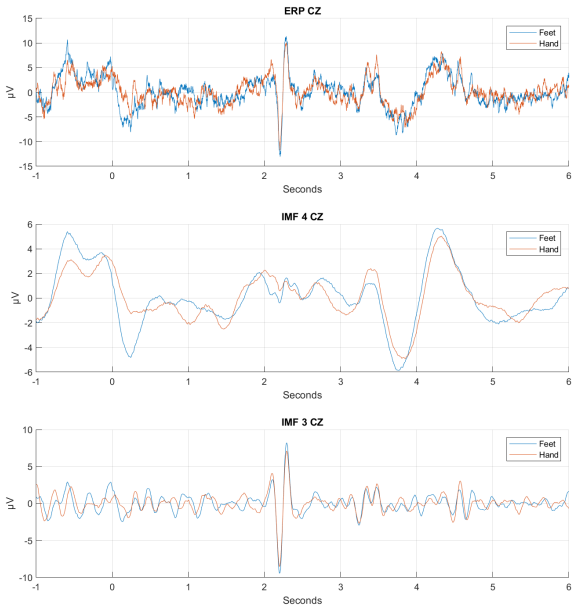

Fig. 3. MVMD result from the ERP for both hand and feet cues of Cz. Only the two last IMFs are shown together with the ERP, with IMF 4 being the final IMF.

III. Results

A. ERP results

The ERP of both right-hand and feet MI movement from subject 4 are presented in Figure 2 and Figure 3 along with the two last IMFs of the MVMD decomposition, composing into four narrowband modes. The plots are from channel C3 and Cz, respectively. Subject 4 was chosen after visual inspection of the subjects and their resulting IMFs, as this subject in our opinion had the most visually interesting results.

The PSD of the ERPs and the two last IMFs are plotted in Figure 4 and Figure 5.

The STFT of the ERPs and the IMFs are plotted in Figure 6 and Figure 7.

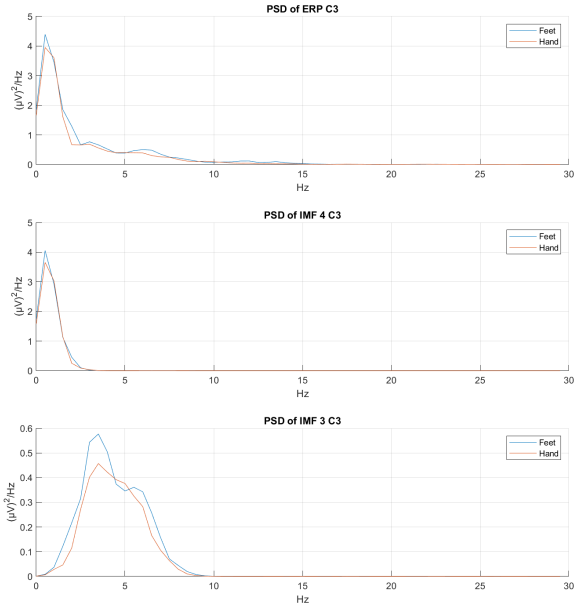

Fig. 4. PSD of the ERP and IMF 3 and 4 from Figure 4 for both hand and feet cues for C3.

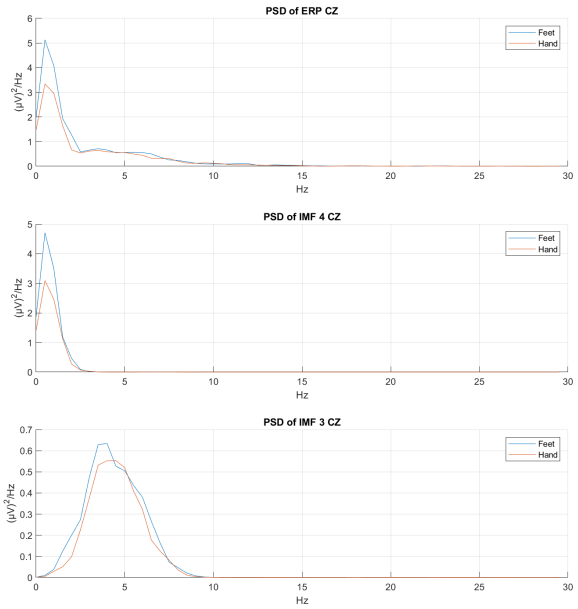

Fig. 5. PSD of the ERP and IMF 3 and 4 from Figure 5 for both hand and feet cues for Cz.

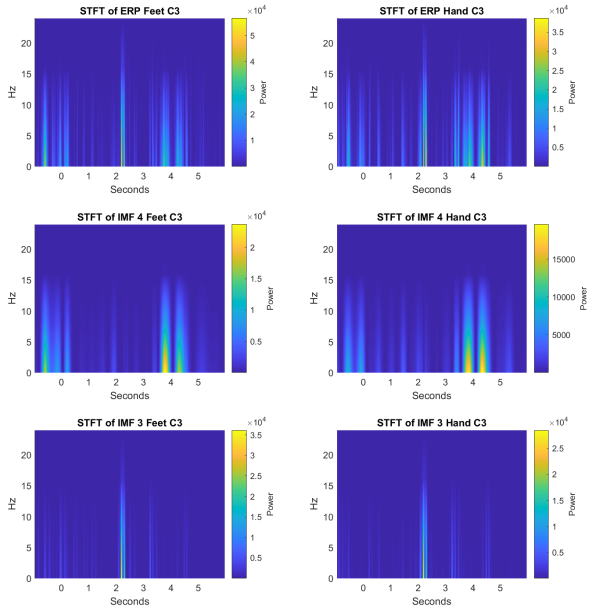

Fig. 6. STFT of the ERP and IMF 3 and 4 from Figure 4 for both hand and feet cues for C3.

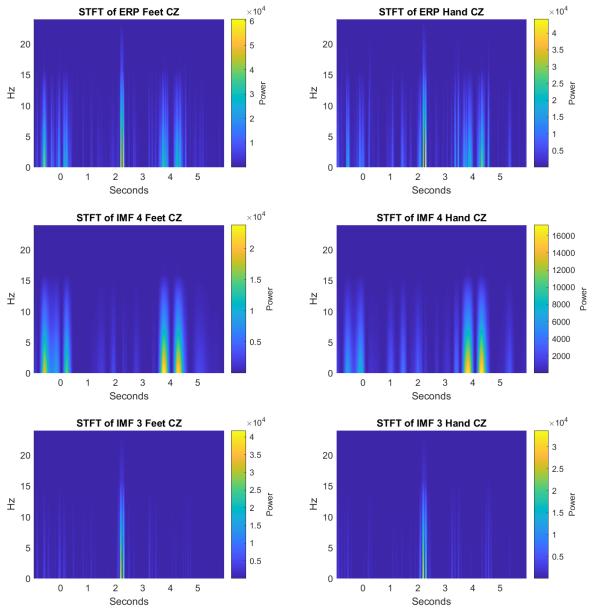

Fig. 7. STFT of the ERP and IMF 3 and 4 from Figure 5 for both hand and feet cues for Cz.

B. ERDS plots of channel 5 (C3), 8 (Cz) and 11 (C4) for subjects 1 and 4

Event-Related Desynchronization and Synchronization is calculated as the percentage change from the baseline. The baseline is the 1 second of activity before the given cue. The orange plot corresponds to right-hand movement, while the blue plot corresponds to feet movement. The plots are divided up by the frequency bands delta (0.5 to 4 Hz), theta (4 to 8 Hz), alpha (8 to 13 Hz) and beta (13 to 30 Hz) though these bands vary somewhat in the literature [21]. The plots are then further divided up by electrode placement, as described in Subsection subsection II-F. The positive y-axis corresponds to synchronization, while the negative corresponds to desynchronization. The hard drawn lines are the averages between all the epochs from all the 5 runs for the subject, while the weaker shaded colors corresponds to a single or a few epochs. The more shaded color in the plot, the larger the variation between epochs. Figure Figure 8 show channels 5 (C3), 8 (Cz) and 11 (C4) for Subject 1. While Figure Figure 9 is the same plot for Subject 4.

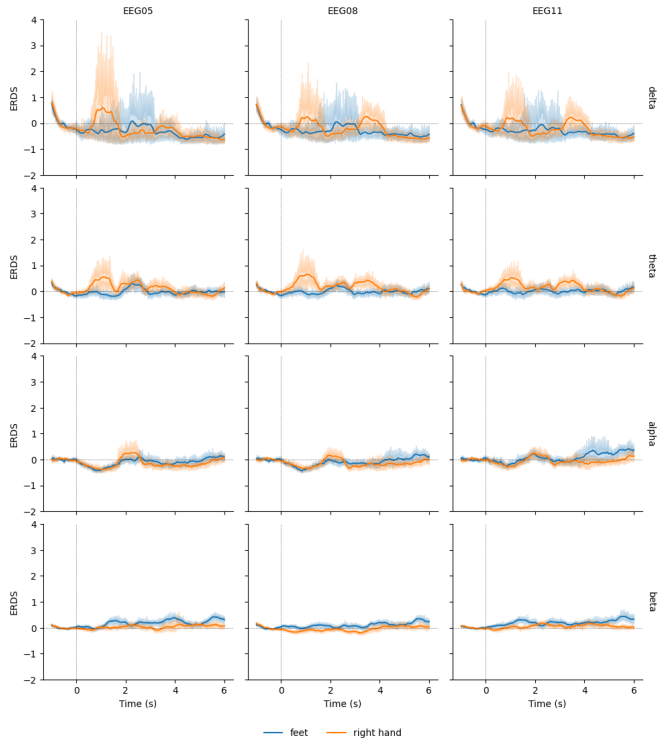

Fig. 8. ERDS for Subject 1 for channels 5 (C3), 8 (Cz) and 11 (C4) for the different frequency bands.

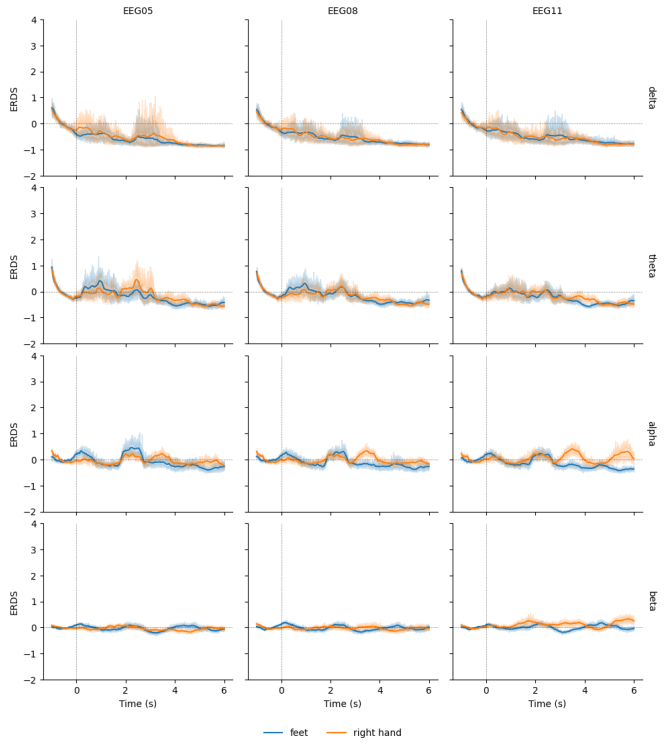

Fig. 9. ERDS for Subject 4 for channels 5 (C3), 8 (Cz) and 11 (C4) for the different frequency bands.

C. ERDS plots averaged between subjects

All the figures from Figure 10 through Figure 14 show all channels averaged over epochs from all subjects and runs.

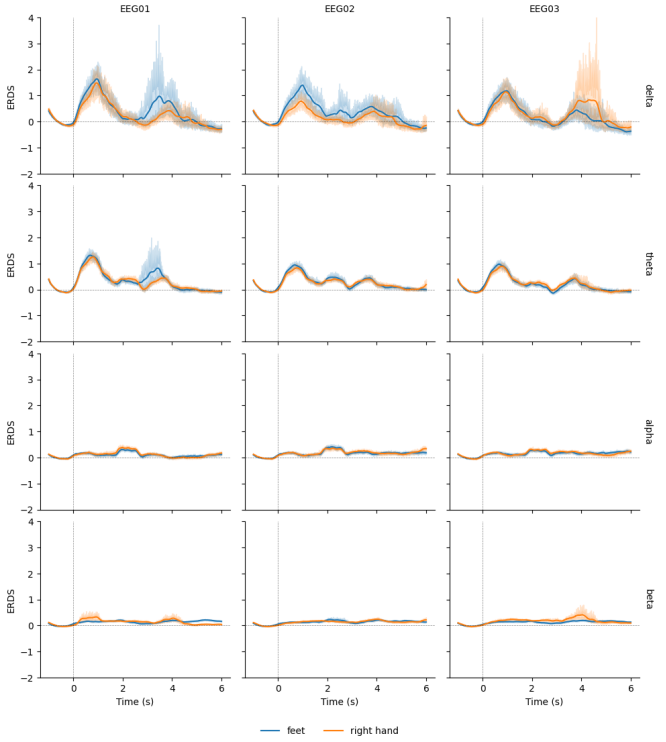

Fig. 10. ERDS averaged over all subjects and all epochs for channels 1, 2 and 3 for the different frequency bands.

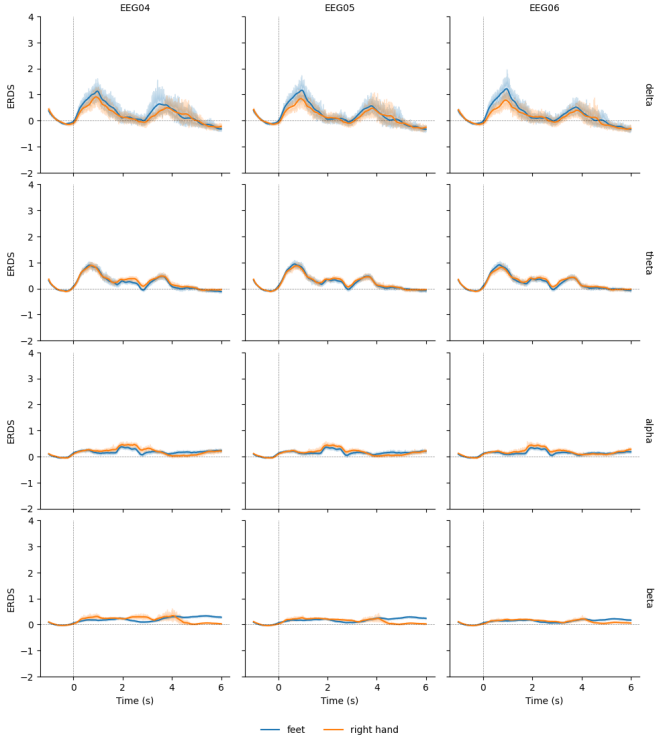

Fig. 11. ERDS averaged over all subjects and all epochs for channels 4, 5 and 6 for the different frequency bands.

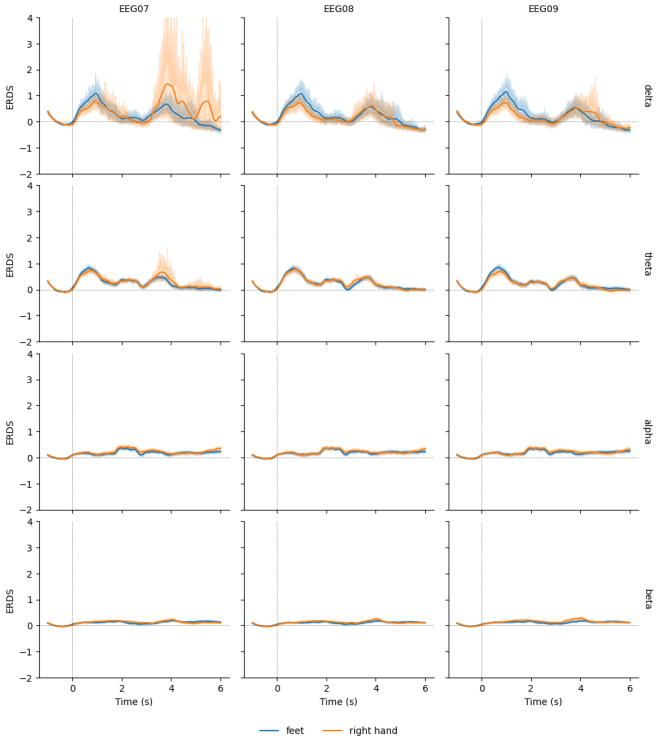

Fig. 12. ERDS averaged over all subjects and all epochs for channels 7, 8 and 9 for the different frequency bands.

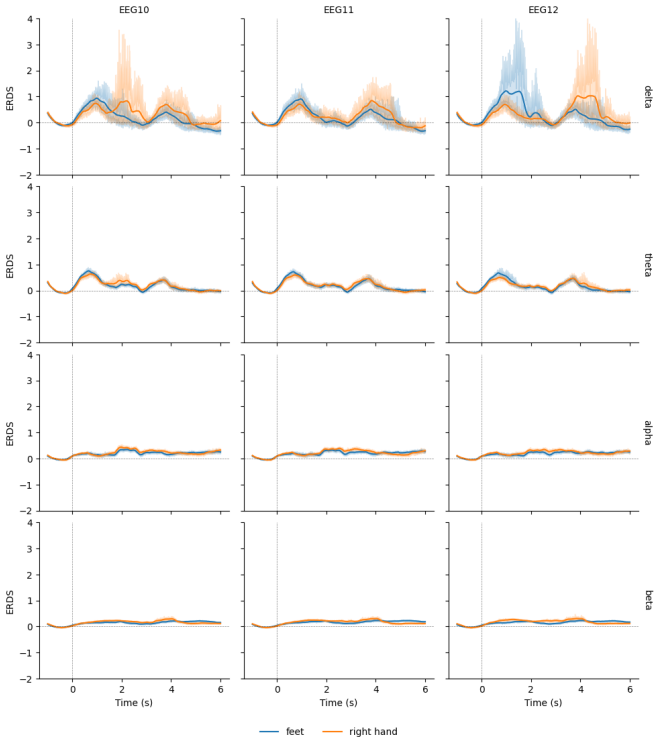

Fig. 13. ERDS averaged over all subjects and all epochs for channels 10, 11 and 12 for the different frequency bands.

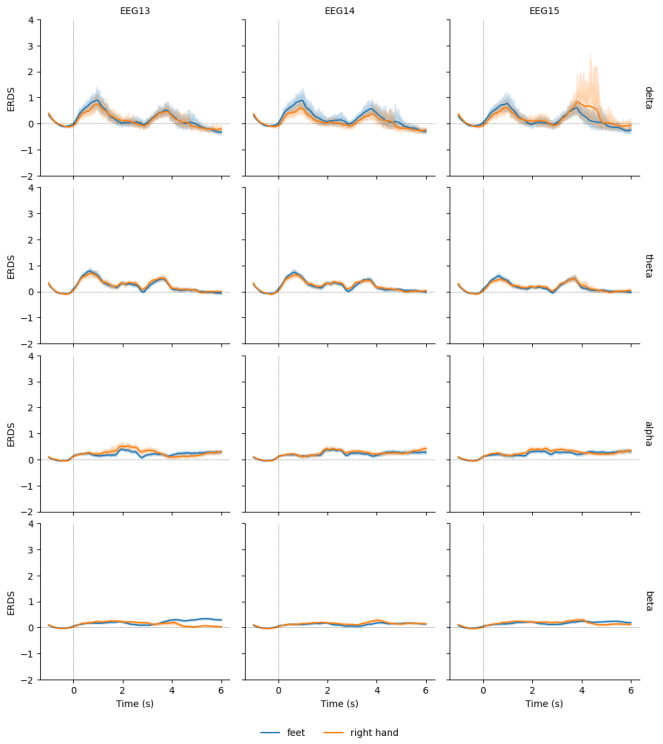

Fig. 14. ERDS averaged over all subjects and all epochs for channels 13, 14 and 15 for the different frequency bands.

IV. Discussion

A. ERP Analysis

The result from the MVMD of the ERPs can be seen in Figure 2 and Figure 3 for respectively channel C3 and Cz for Subject 4. The MVMD analysis found that splitting into four narrowband modes, and thereby IMFs, gave the best result. The two first IMFs mainly consisted of noise and are therefore not included in the figures. IMF 3 for both channels seem to include some of the higher frequencies, especially seen in the spike at just after 2 seconds. IMF 4 looks like a de-noised version of the ERP, containing all the major information. Together with IMF3, these two IMFs provides enough information for analysis of the ERPs. Further analysis is carried out by taking the PSD and the STFT of the ERPs and IMFs. Both methods are used as they both have their strengths, as PSD is a great measure of similarity for the frequency content of the signals, and the STFT is a time-frequency analysis tool that allow to analyze the frequencies in the time domain.

Examining the PSD for both C3 and Cz in Figure 4 and Figure 5 respectively, further supports the observation that the majority of the information is contained within the final IMF seems to be correct. The PSD of the ERP and the IMF4 looks almost identical, meaning that almost all major frequency components are present in the lowest frequency range. Analyzing the PSD of IMF 4 and of the ERP and comparing between channel C3 and Cz, it can be seen that right-hand MI movement are strongest in C3, located at left side of the brain, while feet movement are strongest for Cz,

located in the middle of the brain. From the PSD of IMF3, for both C3 and Cz, the highest power stems from the feet movement.

In C3, the power of the feet and hand ERPs are almost identical for the PSD of IMF4, while the difference in power is greater for the IMF3. The MVMD algorithm almost manages to split the ERP into the delta and theta frequency band. IMF 4 has its frequencies from 0.5 to around 2.5 Hz, while the delta band range from 0.5 to 4 Hz. IMF 3 has mostly frequencies ranging from 2.5 to 8 Hz, corresponding pretty well to the theta band (4 to 8 Hz). This indicates that it is easier to distinguish between hand and feet movements in the theta band, due to greater power difference between the two classes.

Looking at the STFT of C3 and Cz, respectively, in Figure 6 and Figure 7, the frequencies can be analyzed in the time domain. That the STFT of IMF4 and the ERP looks almost identical, supports the observation that most of the frequency components of the ERP are preserved in the IMF4. Looking at the STFT of IMF3, there is a distinct peak just after 2 seconds for both hand and feet at both channels. This distinct peak is also present in the STFT of the ERPs, but not in the STFT of IMF4. From the ERPs in Figure 2 and Figure 3, the faster oscillations are extracted into IMF3, and the same distinct oscillation can be seen just after two seconds. IMF4 looks like a de-noised version of the ERP and can be used for analysis of the delta band, while IMF3 can be used for analysis in the theta band.

B. ERDS Analysis

Many studies in the literature focus on the C3, Cz, and C4 electrodes, which in the data set used are electrodes 5, 8 and 11 respectively.

As found in the literature, large inter-subject variation is also found in this analysis [22] [23]. The ERDS analysis on channel 5, 8 and 11 is almost polar opposites for subject 1 and 4 in both the delta and theta frequency bands. While Subject 1 has some peaks in synchronization for both hand and feet, Figure 8, Subject 4 has a more continuous desynchronization throughout the period, Figure 9. For some channels there is also high intra-subject variation between one subject's different epochs as can be seen from the light shaded colors around the average hard-plotted lines in for example channel 5, 8 and 11 in the delta band for subject 1, Figure 8.

Another finding is that the changes in the alpha and beta frequency bands are mostly insignificant when seen from the ERDS perspective. Though some changes can be seen in some subjects, when averaging across all subjects these bands mostly flatten out. This can be seen in all the averaged plots from Figure 10 to Figure 14. This result is to be expected as it relates to the negative correlation between the frequency of the brain oscillations and their amplitudes as shown in [14].

Another interesting finding is that for most channels there seems to be two spikes in synchronization in the delta and theta bands at about 1s and at 3.5s-4s. This seems to be on average a spike for both feet movement and right-hand movement, though this is highly variable across subjects. This can be seen for most channels in the averaged plots like in Figure 11. The timing spikes are also compliant with earlier findings. [14]

For some channels like 3, 7, 10, 12, 15 there seems to be more synchronization for the right hand than in other channels for the latter peak, as well as more variation (shaded color) as seen in Figure 10, Figure 12, Figure 13 and Figure 14. These channels, except for channel 7, are mostly situated on the right side of the head associated with the left hand, which is unexpected.

From ERDS plots, it is hard to clearly distinguish between the right-hand and feet, even from electrodes placed over the left hemisphere. This indicates that the method of comparison used is not sufficient for separation. Other methods, like direct electrode comparisons of ERDS as used in the paper by Giri [24], might therefore be more beneficial and should be further explored for feet as well.

V. Future work

Future studies should focus on analysis of the unexpected lateralization effects observed in the ERDS findings. This involves examining the synchronization patterns in channels located on the right side of the head and their relationship with right-hand movements.

Another possibility is investigating strategies to overcome the challenges posed by inter- and intra-subject variability in the MI signals. Research into methods that can effectively generalize across different subjects, would be a large contribution to the field.

Given the complex nature of EEG data, applying deep learning models, particularly Convolutional Neural Networks (CNNs), could offer significant improvements in classifying MI signals. Future studies could explore the integration of classical time-frequency analysis results with deep learning models for enhanced performance.

VI. Conclusion

This study's analysis of Motor Imagery (MI) signals using time-frequency methods highlights the significant subject-specific variations in EEG data. Key findings from the Multivariate Variational Mode Decomposition (MVMD) of Event-Related Potentials (ERPs) indicate that lower frequency ranges contain crucial information for analyzing motor movements. However, the variability observed across subjects underscores the challenge of generalizing these findings.

The ERDS analysis points to significant inter- and intra-subject differences, particularly in the delta and theta frequency bands. While changes in the alpha and beta bands were less important.

The study's revelations about synchronization spikes in certain frequency bands and the unexpected findings regarding lateralization (e.g., channels on the right side of the head associated with left-hand movements synchronizing for right-hand movement) offer new avenues for further research.

In summary, this research offers new insights into the complex nature of MI signals, emphasizing the need for personalized approaches in their analysis and application. It also proves the usefulness of classical Time-Frequency Analysis tools. These findings are particularly relevant for the development of brain-computer interfaces and rehabilitation

technologies, highlighting the potential for further research in this domain.

REFERENCES

[1] H. M. Sisti, A. Beebe, M. Bishop, and E. Gabrielsson, "A brief review of motor imagery and bimanual coordination," *Frontiers in Human Neuroscience*, vol. 16, 2022.

[2] C. Schuster, R. Hilfiker, O. Amft, A. Scheidhauer, B. Andrews, J. Butler, U. Kischa, and T. Ettlin, "Best practice for motor imagery: a systematic literature review on motor imagery training elements in five different disciplines," *BMC Med*, vol. 9, no. 75, 2011.

[3] S. M. Christensen, N. S. Holm, and S. K. Puthusserypady, "An improved five class mi based bci scheme for drone controlling using filter bank csp," *2019 7th International Winter Conference on Brain-Computer Interface (BCI)*, pp. 1–6, 2019.

[4] A. Zancanaro, G. Cisotto, J. R. Paulo, G. Pires, and U. J. Nunes, "CNN-based approaches for cross-subject classification in motor imagery: From the state-of-the-art to DynamicNet," in *2021 IEEE Conference on Computational Intelligence in Bioinformatics and Computational Biology (CIBCB)*. IEEE, oct 2021. [Online]. Available: https://doi.org/10.1109%2Fcibcb49929.2021.9562821

[5] J. Kalcher and G. Pfurtscheller, "Discrimination between phase-locked and non-phase-locked event-related eeg activity," *Electroencephalography and Clinical Neurophysiology*, vol. 94, no. 5, pp. 381–384, 1995. [Online]. Available: https://www.sciencedirect.com/science/article/pii/0013469495000406

[6] V. Kolev and J. Yordanova, "Analysis of phase-locking is informative for studying event-related eeg activity," *Biological cybernetics*, vol. 76, no. 3, p. 229–235, 1997. [Online]. Available: https://doi.org/10.1007/s004220050335

[7] A. Mouraux and G. D. Iannetti, "Across-trial averaging of event-related eeg responses and beyond," *Magnetic Resonance Imaging*, vol. 26, no. 7, pp. 1041–1054, 2008.

[8] S. Sur and V. K. Sinha, "Event-related potential: An overview," *Industrial psychiatry journal*, vol. 18, no. 1, pp. 70–73, 2009.

[9] J. F. Friedman, B. H. Thayer, "Facial muscle activity and eeg recordings: redundancy analysis," *Electroencephalography and Clinical Neurophysiology*, vol. 79, no. 5, pp. 358–360, 1991.

[10] S. Eysenck, "Chapter 7 - how the impulsiveness and venturesomeness factors evolved after the measurement of psychoticism," in *On the Psychobiology of Personality*, R. M. Stelmack, Ed. Oxford: Elsevier, 2004, pp. 107–112. [Online]. Available: https://www.sciencedirect.com/science/article/pii/B9780080442099500087

[11] D. Steyrl, R. Scherer, J. Faller, and G. R. Müller-Putz, "Random forests in non-invasive sensorimotor rhythm brain-computer interfaces: a practical and convenient non-linear classifier," *Biomedizinische Technik. Biomedical engineering*, vol. 61, no. 1, pp. 77–86, 2016.

[12] M. Zhuravlev, M. Novikov, R. Parsamyan, A. Selskii, and A. Runnova, "The objective assessment of event-related potentials: An influence of chronic pain on erp parameters," *Neuroscience Bulletin*, vol. 39, pp. 1105 – 1116, 2023.

[13] W. Yan and Y. Wu, "A time-frequency denoising method for single-channel event-related eeg," *Frontiers in Neuroscience*, vol. 16, 2022.

[14] G. Pfurtscheller and F. Lopes da Silva, "Event-related eeg/meg synchronization and desynchronization: basic principles," *Clinical Neurophysiology*, vol. 110, no. 11, pp. 1842–1857, 1999. [Online]. Available: https://www.sciencedirect.com/science/article/pii/S1388245799001418

[15] N. E. Huang, Z. Shen, S. R. Long, M. C. Wu, H. H. Shih, Q. Zheng, N.-C. Yen, C. C. Tung, and H. H. Liu, "The empirical mode decomposition and the hilbert spectrum for nonlinear and non-stationary time series analysis," *Proc. Royal Soc. A: Math., Phys. Eng. Sci.*, vol. 454, no. 1971, pp. 903–995, Mar. 1998.

[16] K. Dragomiretskiy and D. Zosso, "Variational mode decomposition," *IEEE Transactions on Signal Processing*, vol. 62, pp. 531–544, 2014.

[17] N. u. Rehman and H. Aftab, "Multivariate variational mode decomposition," *IEEE Transactions on Signal Processing*, vol. 67, no. 23, p. 6039–6052, Dec. 2019. [Online]. Available: http://dx.doi.org/10.1109/TSP.2019.2951223

[18] N. ur Rehman, "Multivariate variational mode decomposition (mvmd)," https://www.mathworks.com/matlabcentral/fileexchange/72814-multivariate-variational-mode-decomposition-mvmd, 2023, mATLAB Central File Exchange. Retrieved November 26, 2023.

[19] P. Stoica and R. Moses, *Spectral Analysis of Signals*. Prentice Hall, 2005.

[20] H. Chaurasiya, "Time-frequency representations: Spectrogram, cochleogram and correlogram," *rocedia Computer Science*, vol. 167, pp. 1901–1910, 2020.

[21] N. M. Jadeja, *Frequencies and Rhythms*. Cambridge University Press, 2021, p. 32–39.

[22] J. Ma, B. Yang, W. Qiu *et al.*, "A large eeg dataset for studying cross-session variability in motor imagery brain-computer interface," *Scientific Data*, vol. 9, p. 531, 2022. [Online]. Available: https://doi.org/10.1038/s41597-022-01647-1

[23] G. Huang, Z. Zhao, S. Zhang, Z. Hu, J. Fan, M. Fu, J. Chen, Y. Xiao, J. Wang, and G. Dan, "Discrepancy between inter- and intra-subject variability in eeg-based motor imagery brain-computer interface: Evidence from multiple perspectives," *Frontiers in Neuroscience*, vol. 17, 2023.

[24] A. Giri, L. Kumar, and T. K. Gandhi, "Cortical source domain based motor imagery and motor execution framework for enhanced brain computer interface applications," *IEEE Sensors Letters*, vol. 5, no. 12, pp. 1–4, 2021.